Suborganellar Localization of Mitochondrial Proteins and Transcripts in Human Cells

Anna Smirnova, Ludovic Richert, Alexandre Smirnov, Yves Mély, Ivan Tarassov

Suborganellar localisation of mitochondrial proteins and transcripts in human cells

Smirnova Anna[a], Richert Ludovic[b], SmirnovAlexandre[a], Mély Yves[b], Tarassov Ivan[a]*

[a] UMR 7156 - Molecular Genetics, Genomics, Microbiology (GMGM), University of Strasbourg/CNRS, Strasbourg, France

[b] UMR 7021 - Laboratory of Biophotonics and Pharmacology (LBP), University of Strasbourg/CNRS, Illkirch, France

* corresponding author: UMR 7156 - Molecular Genetics, Genomics, Microbiology (GMGM), University of Strasbourg/CNRS, IPCB, 4 allée Konrad Roentgen, 67000, Strasbourg, France

Tel (+33) 03 68 85 13 62

E-mail: i.tarassov@unistra.fr

Running title: Microscopy of mitochondrial proteins and transcripts

Summary

Mitochondria have complex ultrastructure which includes continuous subcompartments, such as matrix, intermembrane space, and two membranes, as well as focal structures, such as nucleoids, RNA granules and mitoribosomes. Comprehensive studies of the spatial distribution of proteins and RNAs inside the mitochondria are necessary to understand organellar gene expression processes and macromolecule targeting pathways. Here we give examples of distribution analysis of mitochondrial proteins and transcripts by conventional microscopy and the super-resolution technique 3D STORM. We provide detailed protocols and discuss limitations of immunolabelling of mitochondrial proteins and newly synthesised mitochondrial RNAs by bromouridine incorporation and single-molecule RNA FISH in hepatocarcinoma cells.

Key Words: confocal microscopy; colocalisation analysis; RNA in situ hybridisation; immunolabelling; 3D STORM; submitochondrial ultrastructure

1. Introduction

Mitochondria are key players in a number of fundamental processes in eukaryotic cells. These organelles, despite their small size (250-500 nm in diameter), have a complex ultrastructure, which includes the outer membrane that surrounds mitochondria and forms contacts with the endoplasmic reticulum, the highly folded inner membrane with cristae hosting proteins of the respiratory chain, the intermembrane space between them, and the innermost compartment called matrix *(1)*. The mitochondrial matrix contains most metabolic enzymes and all factors required for organellar gene expression, including mitochondrial DNA organized in nucleoids, another specialised subcompartment adjacent to the

mitochondrial nucleoid and referred to as RNA granule, and mitochondrial ribosomes (mitoribosomes). Data on distribution of various RNA-binding proteins and *de novo* synthesised RNA visualised by bromouridine inclusion indicate that RNA maturation and the mitoribosome assembly take place in the RNA granules, making them pivotal structures in the mitochondrial genetic information flow *(2)*. Comprehensive studies on the spatial distribution of proteins and RNAs inside the organelles are necessary to understand mitochondrial gene expression processes which seem to be subject to tight spatio-temporal control *(3)*.

Fluorescence microscopy is a common approach for studies of mitochondrial localisation of molecules of interest. Usually, mitochondria are labelled with organelle-specific Mitotrackers or genetically encoded markers of known submitochondrial localisation, fused with a fluorescent protein or a self-labelling protein tag, e.g. Halo-tag, for live cell imaging *(4)*. Alternatively, they are immunostained with antibodies against specific mitochondrial proteins in fixed cells. Mitotracker dyes are widely used, but their submitochondrial localisation is not clear, although some data indicate that electrochemical potential dependent Mitotrackers most probably accumulate in the intermembrane space *(5)*. Genetic tagging requires time-consuming cloning and cell transfection or creation of genetically modified stable cell lines, and may give rise to mislocalisation artefacts. Free from these limitations, immunolabelling of fixed cells is a robust method; however, the fixation procedure may compromise the organellar ultrastructure. For visualisation of individual mitochondrial transcripts, the most straightforward method is RNA fluorescence *in situ* hybridisation (RNA FISH), which also requires fixation and specific sample treatment which may alter mitochondrial ultrastructure. Alterations at this level can be, and likely often are, overlooked, due to the physical resolution limit of conventional fluorescence microscopy, ~200 and ~500 nm in the lateral and axial directions respectively, which is similar to the diameter of mitochondria *(6)*. It is

important to note that, simultaneous imaging of proteins and transcripts is challenging since RNAs can be degraded in solutions typically used in immunolabelling protocols *(7)*.

A recent breakthrough in super-resolution microscopy techniques permitted to obtain data on subdiffractional organisation of the mitochondrial nucleoid *(8,9)*, the channels of the mitochondrial outer envelope *(10)*, the OXPHOS complexes *(11,12)* and MICOS (mitochondrial contact site and cristae organizing system) *(13)* of the inner envelop. Here we analysed by 3D dSTORM (direct Stochastic Optical Reconstruction Microscopy) distributions of proteins of the outer membrane (TOMM20) and matrix (mitochondrial ribosomal protein mL38 and a matrix enzyme thiosulfate sulfurtransferase/ rhodanese) in immunolabelled hepatocarcinoma cell line HepG2. TOMM20, a subunit of the mitochondrial pre-protein import complex, formed characteristic clusters on the outer membrane, as expected. In contrast, for mL38 and rhodanese the super-resolution approach revealed different distribution patterns, in agreement with their localisation in the inner mitochondrial compartment. Whereas mL38 was clustered in distinct foci corresponding to mitoribosomes, rhodanese densely and uniformly filled the mitochondrial matrix. Due to the diffraction limit, this spatial information was not available on images obtained by conventional microscopy (Fig. 1).

Total mitochondrial RNA is often tracked by immunolabelling of bromouridine incorporated in newly synthesised transcripts *(14)*. Information about the copy number and subcellular localisation of individual transcripts can be obtained by RNA FISH. Battich et al. visualised ten mitochondrial mRNAs in human cells using the robust single-molecule RNA branched DNA amplification FISH technology (smRNA bDNA FISH) *(15)*. Besides mRNAs, mitochondrial transcription from two strands of circular mitochondrial DNA gives rise to two ribosomal rRNAs, 22 tRNAs and a few noncoding RNAs. The function and fate of these noncoding RNAs, which are transcribed mainly in antisense to canonical genes (and therefore

often referred to as "mirror" RNAs), are still not clear *(16)*. We found that smRNA bDNA FISH can be adapted for the detection and quantification of mitochondrially encoded rRNAs, low-abundance noncoding RNAs, and even short transcripts like tRNAs. We applied this technology for imaging the *MT-CYB* mRNA, the mitochondrial 12S rRNA, the mitochondrial tRNA[Val], and the mirror RNAs for *MT-CYB* and 12S rRNA *(17,18)*. As expected, 12S rRNA and tRNA[Val] (which is not only a transfer RNA but also a structural component of the mitoribosome *(19)*), were very abundant and nearly filled the entire mitochondrion (Fig. 2A,B). By contrast, mirror-12S and mirror-MT-CYB (also known as lncCYB) RNAs were detected as relatively sparse and distinct spots (Fig. 2A,C). It has been proposed that some mitochondrial mRNAs and their mirror-RNAs may hybridise *in vivo*, especially when the latter are not efficiently degraded by mitochondrial RNA degradosome *(20,21)*. However, our data indicate that under normal conditions the *MT-CYB* mRNA and its antisense counterpart have distinct spatial localisations (Fig. 2C), suggesting that mirror-MT-CYB is not permanently duplexed with the *MT-CYB* mRNA and may play other roles in mitochondrial gene expression.

Finally, we studied distributions of macromolecules in samples treated for combined visualisation of proteins and transcripts by immunostaining and smRNA bDNA FISH. In contrast to the classical immunolabelling procedure, we found that the mitochondria in samples treated for smRNA bDNA FISH, although exhibiting normal shape on confocal images, had distorted ultrastructure revealed by super-resolution microscopy. The distribution of the TOMM20 clusters was clearly affected (Fig. 3, compare with Fig. 1), indicating a limited utility of such a protocol for the joint protein/RNA observation inside mitochondria. However, the smRNA bDNA FISH remained instrumental in the analysis of transcript colocalisation with focal submitochondrial compartments, such as RNA granules and nucleoids, which are clearly distinguishable on a diffraction-limited level and do not seem to

suffer from the treatment. We found that the *MT-CO1* and *MT-CYB* mRNAs appear as distinct foci which are partially colocalised with RNA granules (Fig. 4A, B). Similarly, a portion of 12S rRNA colocalises with the RNA granules, here labelled with antibodies to the RNA-binding protein GRSF1, involved in RNA processing (Fig. 4C). These observations corroborate data on the role of RNA granules in mitochondrial RNA biogenesis and the mitoribosome assembly. Interestingly, the much less abundant noncoding mirror-12S rRNA was detected as foci distinct from RNA granules, suggesting a function unrelated to the mitochondrial RNA biogenesis and mitoribosome assembly (Fig. 4D). Besides the spatial information, smRNA bDNA FISH provides a robust means to evaluate the relative abundance of mitochondrial transcripts between conditions, as recently shown for 12S rRNA, tRNA^{Val} and two mitochondrial mRNAs in normal and knockout HEK293T-Rex cells lacking the mitoribosome biogenesis factor YBEY *(18)*.

Here we provide detailed protocols for immunolabelling of mitochondrial proteins and bromouridine-incorporating newly synthesised mitochondrial RNAs and single-molecule RNA FISH in HepG2 cells. The pipelines for image acquisition by confocal microscopy and 3D dSTORM and subsequent image analysis, including quantitative colocalisation analysis, are also provided.

2. Materials

2.1 Preparation of human cells and their transfection

1. Hepatocarcinoma cell line HepG2

2. Dulbecco's modified Eagle's medium (DMEM) powder with 4.5 mg/mL glucose, sodium pyruvate (110 mg/L), and L-glutamine (Sigma-Aldrich)

3. Fetal bovine serum (FBS) (GIBCO)

4. Streptomycin, penicillin (10,000 U/mL) (Sigma-Aldrich)

5. Amphotericin B Fungizone, 100× solution (Gibco)

6. Sodium bicarbonate powder (Sigma-Aldrich)

7. Uridine in powder (Sigma-Aldrich)

8. Trypsin-EDTA (0.05 %) phenol red solution (Thermo Fisher Scientific)

9. 8-well Nunc Lab-Tek slides N 1 with cover glass bottom (Thermo Fisher Scientific) (*see* **Note 1**)

10. Transfection reagent Lipofectamine 2000 (Invitrogen)

11. OptiMEM Reduced Serum medium for transfection (Gibco)

12. Dulbecco's phosphate buffered saline without $CaCl_2$ (PBS) (Sigma-Aldrich)

2.2 Cell fixation, permeabilization and immunolabelling

1. Paraformaldehyde in powder (Sigma-Aldrich)

2. PBS (Sigma-Aldrich)

3. DMEM (Sigma-Aldrich)

4. Triton X-100 (Sigma-Aldrich)

5. Bovine serum albumin (BSA) (Euromedex)

6. Primary antibodies

7. Secondary antibodies conjugated with fluorescent dyes from the Alexa Fluor or ATTO families (Thermo Fisher Scientific)

8. Prolong Gold (Invitrogen) mounting media

2.3 Labelling of mitochondrial RNA granules by bromouridine inclusion into newly synthesised transcripts

1. 5-bromouridine (Sigma-Aldrich)

2. 5-bromouridine antibodies N 11170376001 (Sigma-Aldrich) or analogous

2.4 Immunolabelling and single molecule RNA is situ hybridization

1. ViewRNA ISH Cell assay kit (Thermo Fisher Scientific)

2. A gene-specific oligonucleotide target probe set. The probe set is designed and purchased directly from the manufacturer (Thermo Fisher Scientific). Depending on the length of the target RNA, it contains 2-to-40 probe pairs binding to the target RNA sequence

3. Prolong Gold mounting media (Invitrogen)

2.5 Conventional confocal microscopy: image acquisition, processing and colocalisation analysis

1. Immersol Immersion Oil 518F (Carl Zeiss)

2.6 dSTORM: sample preparation, image acquisition and processing

1. Sodium borohydride powder (Sigma Aldrich)

2. TetraSpeck beads 100 nm (T7279, Invitrogen)

3. Gold nanoparticles 100 nm, stabilized suspension in 0.1 mM PBS (753688, Sigma-Aldrich)

4. Secondary antibodies conjugated with Alexa Fluor 647

5. Vectashield mounting medium (H-1000, Vector Laboratories)

6. 12-well cell culture plate

7. High precision 18 mm round cover glasses thickness N 1.5H (Marienfeld GmbH)

8. 70% and 100% ethanol

3. Methods

3.1. Preparation of human cells and transfection

1. Reconstitute fresh DMEM medium from the powder (for 1l preparations) by diluting it in 875 mL of milliQ water and adding 10 mL of 100× streptomycin/penicillin, 10 mL of fungizone, 5 mL of 2g/L uridine stock prepared from powder, 100 mL of FBS (decomplemented at 55°C for 40 min) and 3.7 g of sodium bicarbonate. Sterilize medium by filtration *via* a 0.22 μm filter (*see* **Note 2**). Defreeze and cultivate HepG2 cells in DMEM medium in common plastic flasks at 37°C, 5% CO_2 until the cells reach confluency.

2. Wash the confluent cells twice with PBS. Add trypsin-EDTA to the flask and incubate for 4 min at room temperature. Verify under microscope that the cells have become spherical. Add the same volume of the DMEM medium to stop the trypsin action. Seed the detached cells on an 8-well Nunc Lab-Tek slides (Thermo Fisher Scientific) at ~10-15 % density (0.1-0.15 cm^2 per 0.8 cm^2 well) 24-to-48 h prior fixation (*see* **Note 3**). To achieve a homogeneous cell distribution, first add the cell suspension and then the medium to the final volume of 300 μL. Verify under a light microscope that the cell suspension is homogeneous and the cell density is low. Always transfer Lab-Tek slides in the plastic support to avoid the bottom breakage.

3. If the protein of interest is to be detected with antibodies to a tag, *e.g.* the FLAG tag, perform transient transfection of cells to enable the expression of the recombinant protein. For this, dilute 150 ng of plasmid DNA in 50 μL of OptiMEM. In another tube, mix 0.5 μL of Lipofectamine 2000 with 50 μL of OptiMEM by pipetting and incubate for 5 min at room temperature. Mix these two preparations by pipetting and incubate for 20 min at room temperature. Aspirate the medium from the well and at the same time add 200 μL of OptiMEM medium. Accomplish this simultaneously by using a disposable pipette for medium aspiration and an automatic pipette for introduction of the new OptiMEM medium ("two-hands method", *see* **Note 4**). Add 100 μL of the premixed DNA-lipoplex complex in OptiMEM and incubate the cells during 4-to-6 h at 37°C, 5% CO_2. After that, change the medium to DMEM and cultivate cells for ~24 h.

3.2 Cell fixation, permeabilization and immunolabelling

1. Before fixation, verify under a light microscope that the cell density is optimal, i.e. the cell culture is not confluent and single cells are well visible.

2. For preparation of the formaldehyde fixation solution, first prepare a stock solution of 4% formaldehyde in PBS. For this, dissolve paraformaldehyde powder in PBS by heating at 60°C under constant stirring. When paraformaldehyde is fully dissolved, wait until it cools down to room temperature, and then filter through a 0.22 µm filter (*see* **Note 5**).

3. Adjust the concentration of formaldehyde by diluting it with the DMEM medium and heat the fixator to 37°C just before fixation. Aspirate the cultivation medium and 300 µL of the fixator. Fix cells by incubation with the fixator during 12 min at 37°C.

4. Wash the samples five times with PBS gradually increasing the intervals between washes up to 15 minutes: do the second wash immediately after the first one, the third after a 5-min incubation, the forth after a 10-min incubation, and the last one after a 15-min incubation at room temperature.

5. For preparation of the permeabilization solution, add Triton X-100 to PBS (0.5 % v/v) and sonicate for 30 min. This solution should be prepared freshly.

6. Incubate the cells with the permeabilization solution for 10 min at room temperature.

7. Wash the samples with PBS five times.

8. To block the samples, incubate them with 5% BSA in PBS for 30 min at room temperature.

9. Incubate the samples with primary antibodies diluted in the blocking buffer for 1-to-3 h.

10. Wash the samples five times with PBS.

11. Incubate the samples with appropriate secondary antibodies conjugated with fluorophores. To avoid channel cross-talk we recommend to use the combination Alexa Fluor 647 and Alexa

Fluor 488 for two-colour labelling experiments. For Alexa Fluor-conjugated antibodies use a 1:1,000 dilution.

12. Wash the samples five times with PBS.

13. Aspirate PBS and add a few droplets of the Prolong mounting media.

14. The samples can be stored at $4^{\circ}C$ in darkness until the microscopy analysis.

3.3 Labelling of mitochondrial RNA granules by bromouridine incorporation in newly synthesized transcripts

1. Prepare Lab-Tek slides with cells as described in 3.1.

2. Add 5 mM 5-bromouridine to the cells: for this add 3 µL of a 500 mM stock to the well containing 300 µL of DMEM. Incubate the cells in the presence of 5 mM 5-bromouridine during 1 h.

3. Fix and treat the cells as described in 3.2 for immunolabelling of the newly synthesized mitochondrial RNA. Use primary antibodies to 5-bromouridine.

3.4 Immunolabelling and single molecule RNA is situ hybridization

1. Prepare Lab-Tek slides with cells as described in 3.1.

2. Perform smRNA bDNA FISH or simultaneous smRNA bDNA FISH and protein immunostaining according to the manufacturer's protocol for the ViewRNA ISH Cell assay kit based on the branched DNA technology (Thermo Fisher Scientific) (*see* **Note 6**). Briefly, cells are fixed and immunostained, then fixed again and hybridized with a gene-specific oligonucleotide target probe set containing 2-to-40 probe pairs. Signal amplification is achieved through a series of sequential hybridization steps with pre-amplifier, amplifier and fluorophore-labelled oligonucleotides. On day 1, fix and permeabilize the cells, stain them

with antibodies and perform the first hybridisation with a target probe set according to the manufacturer's protocol.

3. On day 2, perform the sequential signal amplification and labelling with fluorophores according to the manufacturer's protocol. For an 8-well slide, use 100 μL of fixators, antibodies and oligonucleotide solutions per well and 300 μL of solutions for washing between steps.

4. After labelling, change the medium to the Prolong mounting medium and image the slides in 24 h.

3.5 Conventional confocal microscopy: image acquisition, processing and colocalisation analysis

1. Image samples under a confocal microscope with an immersion objective with the highest numerical aperture and the corresponding immersion media to achieve the maximal resolution limited by light diffraction. In our studies, samples were imaged on LSM700 or LSM780 microscopes (Carl Zeiss) using a 63×/1.4 NA oil objective under Immersol Oil 518F. The fluorescent labels were excited at 635 nm (Alexa Fluor 647), 561 nm (Alexa Fluor 555) and 488 nm (Alexa Fluor 488) and their emission was collected (650–750 nm, 570–630 nm, 500–540 nm) with PMT detectors.

2. To improve the quality of images, consider several acquisition parameters: the pixel size (around 100 nm is optimal in this case), the number of scans per image, the scanning speed, the laser power, the gain of PMT.

3. Save files in the original format provided by your microscope manufacturer (.zvi for Zeiss).

4. For quantitative colocalisation analysis, open the files in the Fiji image processing package and recode them to the TIFF format. Each file should contain images from two channels.

5. Make segmentation and quantification of subcellular shapes with the Squassh method in a plugin MosaicSuit in Fiji *(22)*. This plugin provides information on the number, size, and intensity of the objects in each channel and the degree of their overlap, estimated by three different coefficients. It also returns a Pearson coefficient for the area containing subcellular shapes and a quaternary code image depicting overlapping and non-overlapping objects in two channels.

3.6 3D dSTORM: sample preparation, image acquisition, processing

1. Clean round cover glasses N1.5H, diameter 18 mm, with plasma cleaner prior to the experiment to eliminate surface contaminants that generate autofluorescence.

2. Place the plasma-cleaned cover glasses in a 12-well plate. Sterilize the cover glasses with 70% ethanol for 20 min, then wash with 100% ethanol and air-dry.

3. Seed 0.8 cm^2 of HepG2 cells into one well of the 12-well slide (~4 cm^2), as described in 3.1, and adjust the volume in the well to 500 µL with DMEM. Where necessary, perform transfection as above by using 600 ng of plasmid DNA and 2 µL of lipofectamine.

4. Perform cell fixation and washing as described in 3.2.

5. Prepare the quencher 0.1% $NaBH_4$ solution just before the use. Quench the residual autofluorescence of the fixator by incubating the cells with 0.1% $NaBH_4$ for 10 min.

6. Wash away the quencher from the cells with a PBS solution 5 times.

7. Perform permeabilization and immunolabelling, as described in 3.2, or treat the samples for RNA labelling according to 3.4. Use secondary antibodies conjugated with Alexa Fluor 647, which is one of the best commercially available synthetic dyes for STORM imaging. Apply the antibody at a 1:5,000 dilution. Foresee at least 400 µL of each solution for treatment of one well in each procedure. For washing steps, apply 1 mL of each solution.

8. Introduce gold nanobeads (diameter 100 nm) into the samples to use them as fiducial markers for mechanical drift correction. For this, sonicate 10 µL of gold nanobeads during 5 min. Then dissolve them in 90 µL of ice-cold water. Sonicate this suspension for 5 min and dilute it with ice-cold water to 5 mL. Replace the PBS solution in the wells with cells by these beads suspension and incubate for 1 h at 4°C.

9. Before microscopy, wash the samples twice with milliQ water to remove residual salts and then cover the sample with Vectashield medium, which is an optimal medium for blinking of Alexa Fluor 647 to perform single-molecule localisation microscopy *(23)* .

10. 3D STORM microscopy can be performed on any commercial or home-build microscope for single-molecule localization microscopy equipped with an astigmatism modulus. Here we use adaptive optics (MiCAO, Adaptive Optics) to generate this astigmatism. Adaptive optics is also used for point spread function (PSF) optimization. Our studies were made on a home-built setup based on a Nikon Eclipse Ti microscope with 100×/ 1.49 NA oil-immersion objective. Low autofluorescence immersion oil NF2 (Nikon) was use to minimize background. A 642 nm laser (Oxxius) was used for excitation of Alexa Fluor 647. The laser power during the experiments was set to 50 mW at the objective, which resulted in $2\,\mathrm{kW/cm}^2$ excitation intensity at the sample. Emission from the sample was spectrally filtered with the help of a multi-band dichroic mirror (BrightLine quad-edge super-resolution laser dichroic beamsplitter: Di03-R405/488/561/635-t1-25x36, Semrock) and notch filters (StopLine single-notch filters: NF03-561E-25 and NF03-642E-25, Semrock; in order to remove the scattered laser light), and then imaged on an EM-CCD camera with 16×16-µm pixels from Hamamatsu (ImagEM). An additional lens of 1.5× was used to obtain a final magnification of 150× corresponding to a pixel size of 106.67 nm. To limit the Z drift, a Z-stabilization was ensured by the perfect focus system (PFS, Nikon Eclipse Ti) on the microscope.

11. Before sample imaging, perform optimization of the point spread function (PSF) to minimize residual optical aberrations (spherical, coma, etc.). Use adaptive optics (Imagine Optics) and its algorithms to optimize the PSF of immobilized TetraSpeck fluorescent beads in the Vectashield medium.

12. For 3D STORM, use the adaptive optics to introduce astigmatism in order to create an asymmetric PSF. The resulting shape and orientation of the PSF depend now on the z-position of the fluorophores. Acquire a z-scan of the immobilized TetraSpeck fluorescent beads in the Vectashield medium over a 1.4 µm depth to image the shape variation of the PSF as a function of the z-position of emitter.

13. From the z-scan, generate the calibration curve with the ThunderSTORM ImageJ plugin *(24)*. By fitting the PSF with a two-dimensional Gaussian function, two sigma values are obtained from which the z-position of the fluorophore can be determined from the calibration curve.

14. Use low laser intensity settings to choose a region of interest that contains few fiducial beads for mechanical drift correction.

15. To obtain the stack of images of the region of interest, adjust the laser power to high values (2 kW/cm^2) required for the stochastic blinking of fluorophores and adjust time acquisition of the camera to obtain only isolated fluorophore bursts (typically between 10 to 50 ms) and collect 10,000 images of 512×256 pixels.

16. In order to obtain super resolved image, perform image analysis with the ThunderSTORM plugin in Fiji (*see* **Note 7**). The analysis including automated processing, post-filtering, and drift correction generates the sub-diffraction molecular coordinates. These coordinates are then used to obtain the final 3D image with a colour code for the Z-axis position. From this image, a 2D X-Y or X-Z sub-diffraction section image can be selected.

4. Notes

1. Alternatively, slides with removable chambers can be used. In this case, after labelling and chambers removal, apply the Prolong mounting medium in each well, cover the slide with a cover glass thickness N1 and seal with colourless nail polish. Slides with 8 or even more wells are optimal for immunolabelling and RNA FISH since they permit to minimize the volume of the applied reagents and thus reduce the cost. In contrast, the use of classical cover glasses in cell cultivation plates requires high volumes of solutions.

2. Reconstitution of fresh cell cultivation medium from powder guarantees its sterility, correct pH and stability of components.

3. Low cell density is an important prerequisite for the experiments. It enables adequate labelling and imaging of individual cells. Application of trypsin for cell detachment permits obtaining a homogeneous layer of cells on the slide. This procedure should not be replaced by PBS-EDTA cell detachment.

4. We recommend performing the change of solutions for cell samples by the two-hands method: introduce the fresh solution with an automatic pipette by touching the wall in one corner of the well and aspirate the old solution with a disposable plastic pipette from the opposite side. It excludes even a short exposure of cells to air, which may stress them and cause undesirable artifacts.

5. The solution of formaldehyde should not boil during dissolution. The prepared stock can be stored at -20°C for several months. Only freshly thawed aliquots should be used for preparation of the fixator. The described fixator solution should not be replaced by commercial formaldehyde liquid stocks, since they contain methanol for stabilisation. Fixation with such solutions alters mitochondrial ultrastructure.

6. A very detailed step-by-step protocol and a troubleshooting guide is provided by the manufacturer of the ViewRNA ISH Cell assay kit (Thermo Fisher Scientific) (https://www.thermofisher.com/order/catalog/product/QVC0001#/QVC0001).

7. A comprehensive and user-friendly manual for the ThunderSTORM plugin is created by developers *(24)*.

Figure Captions

Figure 1. Conventional and super-resolution microscopy of mitochondrial proteins in immunolabelled HepG2 cells. (**A-C**) 3D STORM images of the outer membrane protein TOMM20 (**A**), the matrix-localised mitochondrial ribosomal protein mL38 (**B**), and the matrix enzyme thiosulfate sulfurtransferase/ rhodanese (**C**) Scale bars are 1 μm. Lower subpanels show a zoom on individual mitochondria. Scale bars are 500 nm. (**D-F**) Confocal images of the same proteins. Scale bars are 10 μm.

Figure 2. Confocal microscopy of mitochondrial RNAs visualised by smRNA FISH in HepG2 cells. (**A**) 12S rRNA (magenta) and its mirror counterpart (green). The lower left panel is merged image. The lower right panel shows a quaternary code image produced by Squassh where 12S rRNA is in red, its mirror counterpart is in green and their overlapping regions are in yellow. (**B**) The mitochondrial tRNA[Val]. (**C**) *MT-CYB* mRNA (magenta) and its mirror RNA (lncCYB) (green). The lower left panel is merged image. The lower right panel shows a quaternary code image

produced by Squassh where the *MT-CYB* mRNA is in red, the lncCYB RNA is in green and their overlapping regions are in yellow. Scale bars are 10 µm.

Figure 3. Super-resolution microscopy of the mitochondrial outer membrane protein TOMM20 in HepG2 cells treated for visualisation of proteins according to smRNA bDNA FISH protocol. Part of a cell (scale bar is 1 µm) and a zoomed image of an individual mitochondrion (scale bar is 500 nm) are shown.

Figure 4. Confocal microscopy of mitochondrial transcripts and RNA granules in HepG2 cells. (**A**) *MT-CO1* mRNA (green) and RNA granules labelled by bromouridine incorporation in newly synthesized transcripts (magenta). A quaternary code image produced by Squassh, where the *MT-CO1* mRNA is in green, RNA granules are in red and their overlapping regions are in yellow, is shown on the right. (**B**) *MT-CYB* mRNA (green) and RNA granules labelled by bromouridine incorporation in newly synthesized transcripts (magenta). (**C**) 12S rRNA (green) and RNA granules labelled by immunostaining of GRSF1 (magenta). The lower left panel is merged image. The lower right panel shows a quaternary code image produced by Squassh where 12S rRNA is in green, RNA granules are in red and their overlapping regions are in yellow. (**D**) Mirror-12S rRNA (green) visualised in the same cells. The lower left panel is merged image. The lower right panel shows a quaternary code image produced by Squassh where the mirror-12S rRNA is in green, RNA granules are in red and their overlapping regions are in yellow. Scale bars are 10 µm.

References

1. Frey TG, Mannella CA (2000) The internal structure of mitochondria. Trends in biochemical sciences 25 (7):319-324. doi:10.1016/s0968-0004(00)01609-1
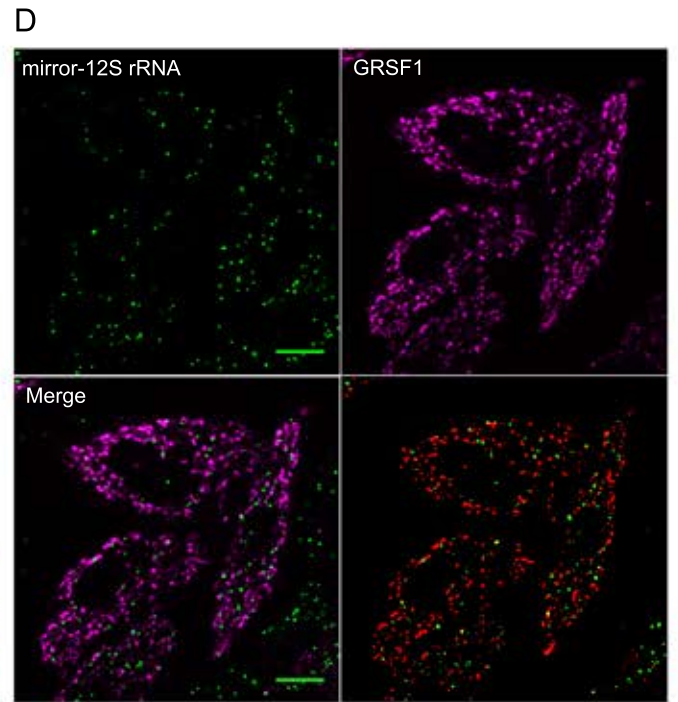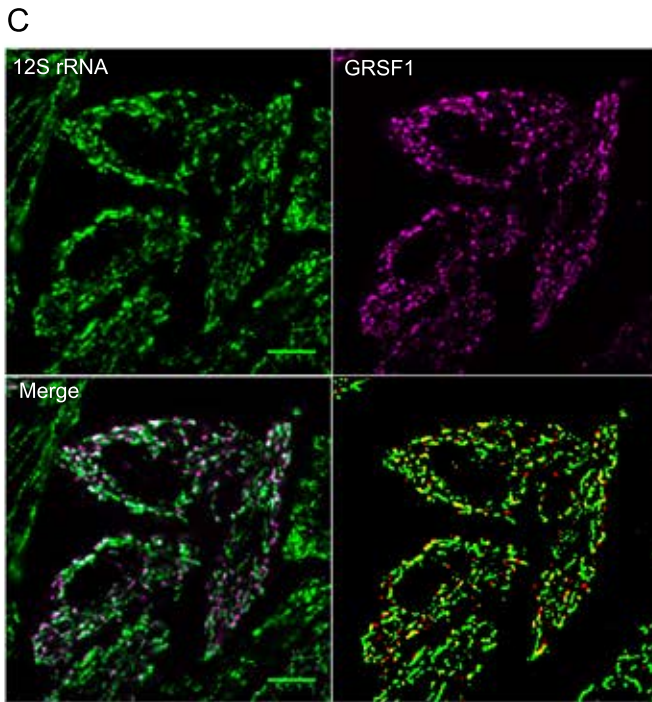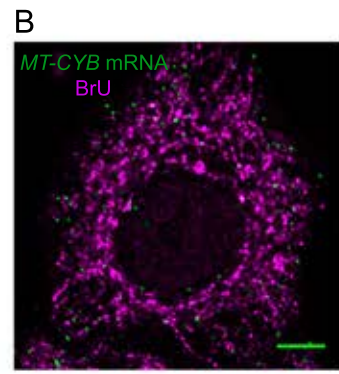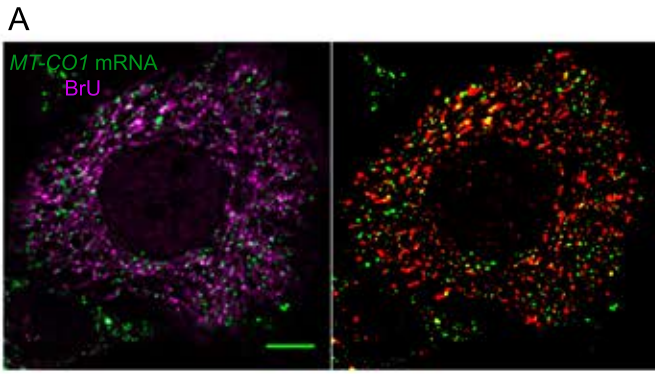
2. Jourdain AA, Boehm E, Maundrell K, Martinou JC (2016) Mitochondrial RNA granules: Compartmentalizing mitochondrial gene expression. The Journal of cell biology 212 (6):611-614. doi:10.1083/jcb.201507125

3. Pearce SF, Rebelo-Guiomar P, D'Souza AR, Powell CA, Van Haute L, Minczuk M (2017) Regulation of Mammalian Mitochondrial Gene Expression: Recent Advances. Trends in biochemical sciences 42 (8):625-639. doi:10.1016/j.tibs.2017.02.003

4. Jakobs S (2006) High resolution imaging of live mitochondria. Biochimica et biophysica acta 1763 (5-6):561-575. doi:10.1016/j.bbamcr.2006.04.004

5. Opstad Ida S, Wolfson Deanna L, Øie Cristina I, Ahluwalia Balpreet S (2018) Multi-color imaging of sub-mitochondrial structures in living cells using structured illumination microscopy. Nanophotonics, vol 7. doi:10.1515/nanoph-2017-0112

6. Jakobs S, Wurm CA (2014) Super-resolution microscopy of mitochondria. Current opinion in chemical biology 20:9-15. doi:10.1016/j.cbpa.2014.03.019

7. Ma B, Tanese N (2017) RNA-Directed FISH and Immunostaining. In: Liehr T (ed) Fluorescence In Situ Hybridization (FISH): Application Guide. Springer Berlin Heidelberg, Berlin, Heidelberg, pp 327-335. doi:10.1007/978-3-662-52959-1_34

8. Kukat C, Wurm CA, Spahr H, Falkenberg M, Larsson NG, Jakobs S (2011) Super-resolution microscopy reveals that mammalian mitochondrial nucleoids have a uniform size and frequently contain a single copy of mtDNA. Proceedings of the National Academy of Sciences of the United States of America 108 (33):13534-13539. doi:10.1073/pnas.1109263108

9. Silva Ramos E, Motori E, Bruser C, Kuhl I, Yeroslaviz A, Ruzzenente B, Kauppila JHK, Busch JD, Hultenby K, Habermann BH, Jakobs S, Larsson NG, Mourier A (2019) Mitochondrial fusion is required for regulation of mitochondrial DNA replication. PLoS genetics 15 (6):e1008085. doi:10.1371/journal.pgen.1008085
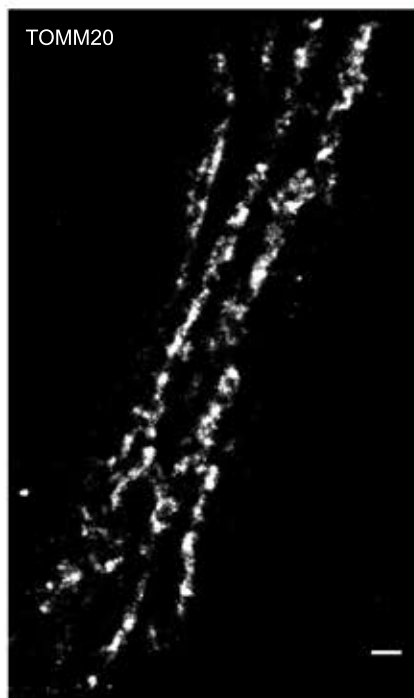
10. Huang B, Jones SA, Brandenburg B, Zhuang X (2008) Whole-cell 3D STORM reveals interactions between cellular structures with nanometer-scale resolution. Nature Methods 5 (12):1047-1052. doi:10.1038/nmeth.1274

11. Stoldt S, Wenzel D, Kehrein K, Riedel D, Ott M, Jakobs S (2018) Spatial orchestration of mitochondrial translation and OXPHOS complex assembly. Nature Cell Biology 20 (5):528-534. doi:10.1038/s41556-018-0090-7

12. Stephan T, Roesch A, Riedel D, Jakobs S (2019) Live-cell STED nanoscopy of mitochondrial cristae. Scientific Reports 9 (1):12419. doi:10.1038/s41598-019-48838-2

13. Jans DC, Wurm CA, Riedel D, Wenzel D, Stagge F, Deckers M, Rehling P, Jakobs S (2013) STED super-resolution microscopy reveals an array of MINOS clusters along human mitochondria. Proceedings of the National Academy of Sciences 110 (22):8936. doi:10.1073/pnas.1301820110

14. Iborra FJ, Kimura H, Cook PR (2004) The functional organization of mitochondrial genomes in human cells. BMC biology 2:9. doi:10.1186/1741-7007-2-9

15. Battich N, Stoeger T, Pelkmans L (2013) Image-based transcriptomics in thousands of single human cells at single-molecule resolution. Nature methods 10 (11):1127-1133. doi:10.1038/nmeth.2657

16. Kotrys AV, Szczesny RJ (2019) Mitochondrial Gene Expression and Beyond-Novel Aspects of Cellular Physiology. Cells 9 (1). doi:10.3390/cells9010017

17. Jeandard D, Smirnova A, Tarassov I, Barrey E, Smirnov A, Entelis N (2019) Import of Non-Coding RNAs into Human Mitochondria: A Critical Review and Emerging Approaches. Cells 8 (3):286. doi:10.3390/cells8030286

18. Summer S, Smirnova A, Gabriele A, Toth U, Mandela F, Förstner KU, Kuhn L, Chicher J, Hammann P, Mitulović G, Entelis N, Tarassov I, Rossmanith W, Smirnov A (2019)

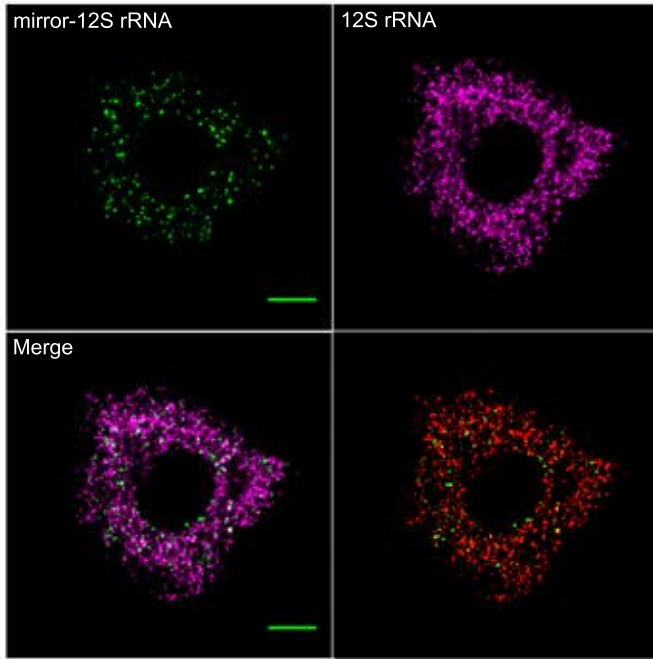YBEY is an essential biogenesis factor for mitochondrial ribosomes. bioRxiv:2019.2012.2013.874362. doi:10.1101/2019.12.13.874362

19. Brown A, Amunts A, Bai X-C, Sugimoto Y, Edwards PC, Murshudov G, Scheres SHW, Ramakrishnan V (2014) Structure of the large ribosomal subunit from human mitochondria. Science 346 (6210):718-722. doi:10.1126/science.1258026

20. Rackham O, Shearwood AM, Mercer TR, Davies SM, Mattick JS, Filipovska A (2011) Long noncoding RNAs are generated from the mitochondrial genome and regulated by nuclear-encoded proteins. Rna 17 (12):2085-2093. doi:10.1261/rna.029405.111

21. Dhir A, Dhir S, Borowski LS, Jimenez L, Teitell M, Rotig A, Crow YJ, Rice GI, Duffy D, Tamby C, Nojima T, Munnich A, Schiff M, de Almeida CR, Rehwinkel J, Dziembowski A, Szczesny RJ, Proudfoot NJ (2018) Mitochondrial double-stranded RNA triggers antiviral signalling in humans. Nature 560 (7717):238-242. doi:10.1038/s41586-018-0363-0

22. Rizk A, Paul G, Incardona P, Bugarski M, Mansouri M, Niemann A, Ziegler U, Berger P, Sbalzarini IF (2014) Segmentation and quantification of subcellular structures in fluorescence microscopy images using Squassh. Nature protocols 9 (3):586-596. doi:10.1038/nprot.2014.037

23. Glushonkov O, Réal E, Boutant E, Mély Y, Didier P (2018) Optimized protocol for combined PALM-dSTORM imaging. Scientific Reports 8 (1):8749. doi:10.1038/s41598-018-27059-z

24. Ovesný M, Křížek P, Borkovec J, Svindrych Z, Hagen GM (2014) ThunderSTORM: a comprehensive ImageJ plug-in for PALM and STORM data analysis and super-resolution imaging. Bioinformatics 30 (16):2389-2390. doi:10.1093/bioinformatics/btu202
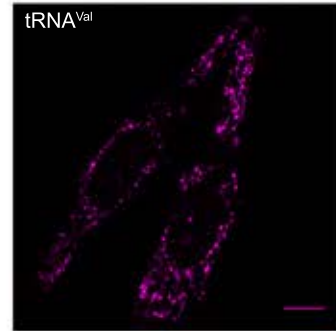
A MT-CO1 mRNA
BrU

B MT-CYB mRNA
BrU

C 12S rRNA | GRSF1
Merge

D mirror-12S rRNA | GRSF1
Merge

TOMM20

A

mirror-12S rRNA | 12S rRNA

Merge

B

tRNA^Val

C

lncCYB RNA | *MT-CYB* mRNA

Merge

A   TOMM20

B   mL38

C   Rhodanese

D

E

F